Design of Structured Surfaces for Directional Mobility of Droplets

Takehito Osada[1], Arata Kaneko[1], Nobuyuki Moronuki[1,#] and Tomoyo Kawaguchi[1]

1 Graduate School of System Design, Tokyo Metropolitan University, 6-6, Asahigaoka, Hino, Tokyo, Japan, 191-0065
Corresponding Author / E-mail: moronuki@tmu.ac.jp, TEL: +81-42-585-8606, FAX: +81-42-583-5119

KEYWORDS: Structured-surface, Sliding angle, Directional mobility

This paper deals with the directional mobility of droplets on structured surfaces. Structured surfaces were micro-patterned with rectangular lines and spaces of varying pitch and height in the sub-millimeter range. The material used was polydimethylsiloxane, which is hydrophobic and wettable by oil. First, we studied the effect of the structural design on the sliding angle of pure water or oil through experiments. For pure water droplets, we found that a wider pitch enhanced the directionality. On the other hand, oil droplets spread along the groove because of their low surface tension and strong capillary force. The directionality of the sliding angle of oil droplets was larger than that of pure water, especially when the groove was narrower and deeper. Second, we poured a large amount of liquid on the structure and evaluated the removal rate on the tilted surface. We found that a parallel structure enhanced the liquid mobility for both pure water and oil.

Manuscript received: October 2, 2007 / Accepted: March 11, 2008

1. Introduction

An appropriate surface microstructure affords superhydrophobic characteristics similar to those of a lotus leaf[1]. The design and manufacture of such surfaces have been previously discussed. Line-and-space (L&S) patterned surfaces have also been studied to provide information on directional wettability[2-6] and to lower the surface flow resistance[7]. Directional mobility of liquids is important for various devices such as vehicle windshields, heat exchangers, and so on.

On a grooved surface, it is well known that liquid moves easily along the grooves. However, previous studies have not clarified the optimum design for such patterned surfaces. In addition, the liquids considered in previous studies have been limited to water droplets with volumes as small as a few microliters in many cases, wherein surface tension is dominant over the effect of gravity. Thus, these results cannot be directly applied when a large amount of liquid is poured on a surface. In some cases, the amount of residual liquid must be minimized because many liquids cannot be removed completely and rapidly after pouring. Therefore, it is necessary to examine the actual design when a large amount of liquid is considered. Issues of durability and physical or geometrical structuring should be considered before chemical modifications.

This paper aims to determine a comprehensive design of surface structures that can disperse liquid easily and rapidly. The relationship between the size of a L&S structure and the directional mobility of the liquid is discussed in detail. First, the sliding angles on a structured surface were obtained. Then, a large amount of liquid was poured on the surface and the residual area was measured to determine the optimum design for quick removal.

2. Basic theories relating to wetting phenomena

Figure 1(a) shows the cross-section of a droplet on a surface. The contact angle θ can be given by Young's equation[8]:

$$\cos\theta = \frac{\gamma_{SV} - \gamma_{SL}}{\gamma_{LV}} \tag{1}$$

where γ_{SV}, γ_{SL}, and γ_{LV} are the interfacial tension per unit length of the solid-vapor, solid-liquid and liquid-vapor interface, respectively. These tensions are determined by the combination of materials used. The γ_{LV} value is large for water (72 mN/m) and small for oil (30 mN/m). The contact angle for oil also tends to be small. Considering the effect of roughness or microstructures, the contact angle can be predicted by Cassie-Baxter's equation, which estimates the wettability as the summation of different parts. For a two-component surface, the contact angle θ' is given as follows[9]:

$$\begin{aligned} \cos\theta' &= f_1 \cos\theta_1 + f_2 \cos\theta_2 \\ f_1 + f_2 &= 1 \end{aligned} \tag{2}$$

where f_1 and f_2 are the fraction of the surface with contact angles of θ_1 and θ_2, respectively. This equation is commonly used when the structure is steep and air is trapped in the groove.

Figure 1(b) shows the force balance at the sliding angle α at which the droplet begins to move[1]:

$$\rho V g \sin\alpha = \gamma_{LV}(\cos\theta_R - \cos\theta_A) \tag{3}$$

where ρ, V, g, θ_R, and θ_A are the density of the liquid, volume of the droplet, gravitational acceleration, receding angle, and advancing angle, respectively. This equation is derived assuming that both the surface tension and hysteresis of the contact angle, which is defined as the difference between the advancing and receding angles, are small to reduce the sliding angle.

On a structured surface, the mechanism of spreading and sliding droplets is much more complicated than on a surface without structures. For example, droplets can be pinned at the edge of the structure. Therefore, these equations cannot be applied directly and an experimental approach is necessary.

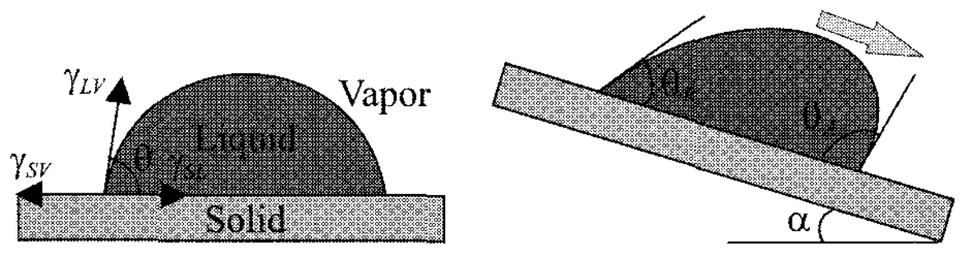

(a) Young's law (b) Sliding angle on a flat surface

Fig. 1 Basic droplet profile models

3. Fabrication of the structure

A surface structure with an L&S pattern was fabricated on polydimethylsiloxane (PDMS). In this study, pure water and oil were used as the liquids. The oil was commercial canola oil with a viscosity of 50 mPa·s. Pure water and oil on a flat surface have contact angles of 107 and 53 degrees and surface tensions of 72 and 30 mN/m, respectively. PDMS is hydrophobic and wettable by oil.

Figure 2 shows the fabrication process for the L&S structure. The L&S structure was fabricated by photolithography. The photoresist, SU-8 (MicroChem), was used as a mold for the subsequent processes. Its thickness was adjusted to 15, 50 and 100 μm. PDMS with 10 wt% of curing agent was cast into the mold and cured in an oven at 343 K for 70 min. The cured PDMS was peeled off from the mold.

Figure 3 shows a scanning electron microscope image of the structure and its cross-sectional profile measured by a laser microscope. The obtained rectangular profile was as intended, although its height was less than the designed height. The design parameters of the structure, the pitch P, width W, and height H, are also defined in the figure. The specifications of the sample structure are summarized in Table 1.

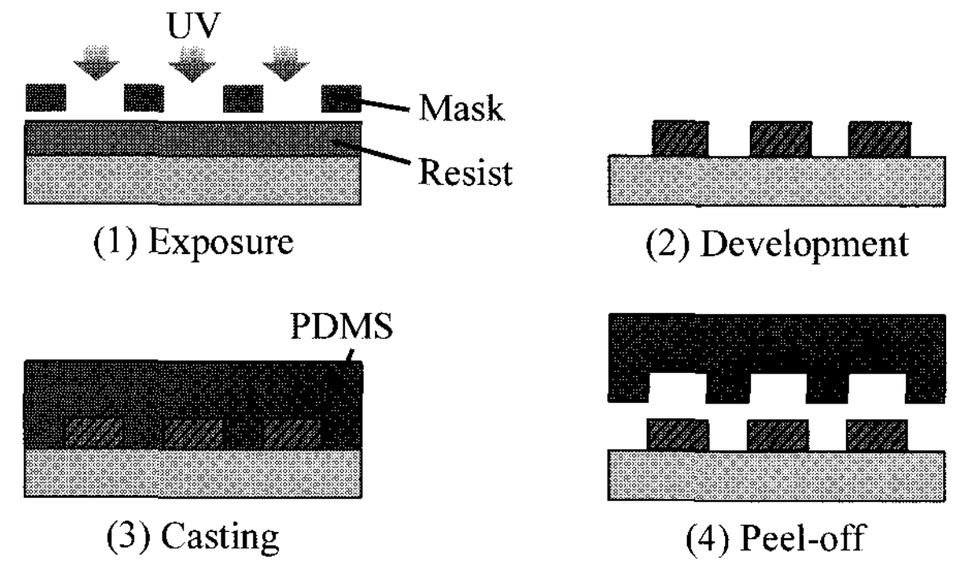

Fig. 2 Process for the L&S structure

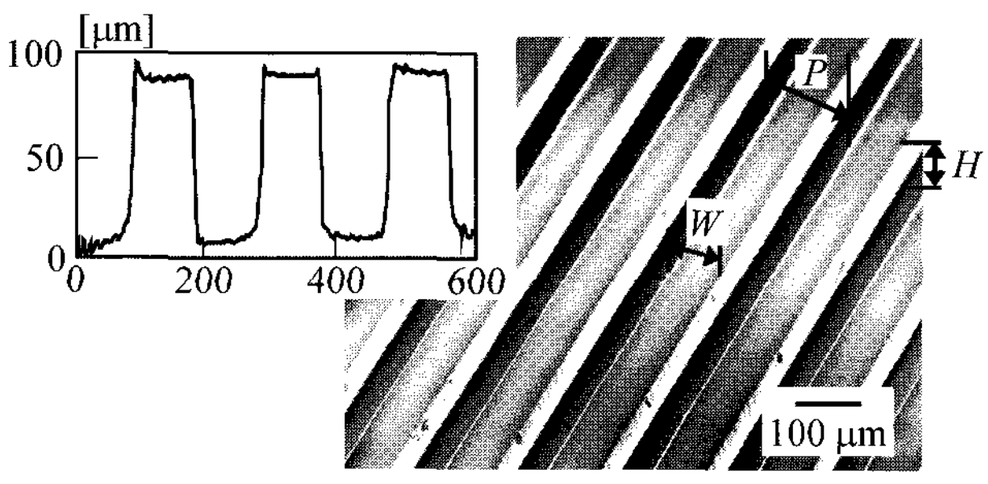

Fig. 3 SEM image of the structure and its cross-sectional profile

4. Experiments

4.1 Sliding angle

The sliding and contact angles were measured with the apparatus

Table 1 Specifications of the L&S structure

No.	Pitch P [μm]	Width W [μm]	Height H [μm]
1	200	100	100
2	400	200	
3	600	300	
4	2000	1000	
5	200	100	50
6			15

shown in Fig. 4. A motorized syringe was used to define the droplet volume, and the shape of the droplet was analyzed by a combination of a charge coupled device (CCD) camera and processing software. The tilt angle was set by inclining the whole system. The L&S structure was set parallel or orthogonal to the inclination. In this study, the sliding angle is defined as the angle at which the receding line of the droplet begins to move.

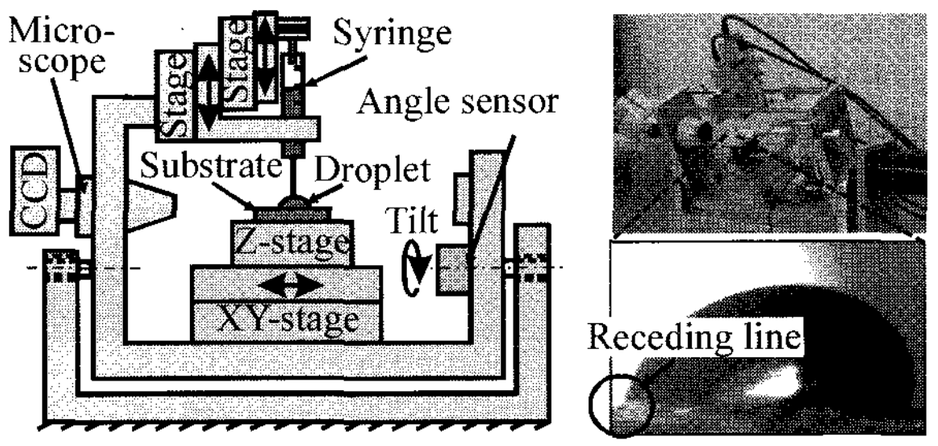

Fig. 4 Apparatus for measuring the contact and sliding angles

Figure 5 shows the relationship between the droplet volume and the sliding angles on L&S Structure No. 1 in Table 1. The sliding angle decreased with increasing volume for water, shown in Fig. 5(a). This is qualitatively explained by Eq. (3), which indicates that the sliding angle was inversely proportional to the volume of the droplet. The directionality was dependent on the sliding direction. A sliding angle orthogonal to the structure was larger than one parallel to the structure because movement across a structure requires much more energy compared to movement along a structure, as shown in Fig. 6[1]. Pinning of the droplet at the edge of the structure also enhanced this tendency.

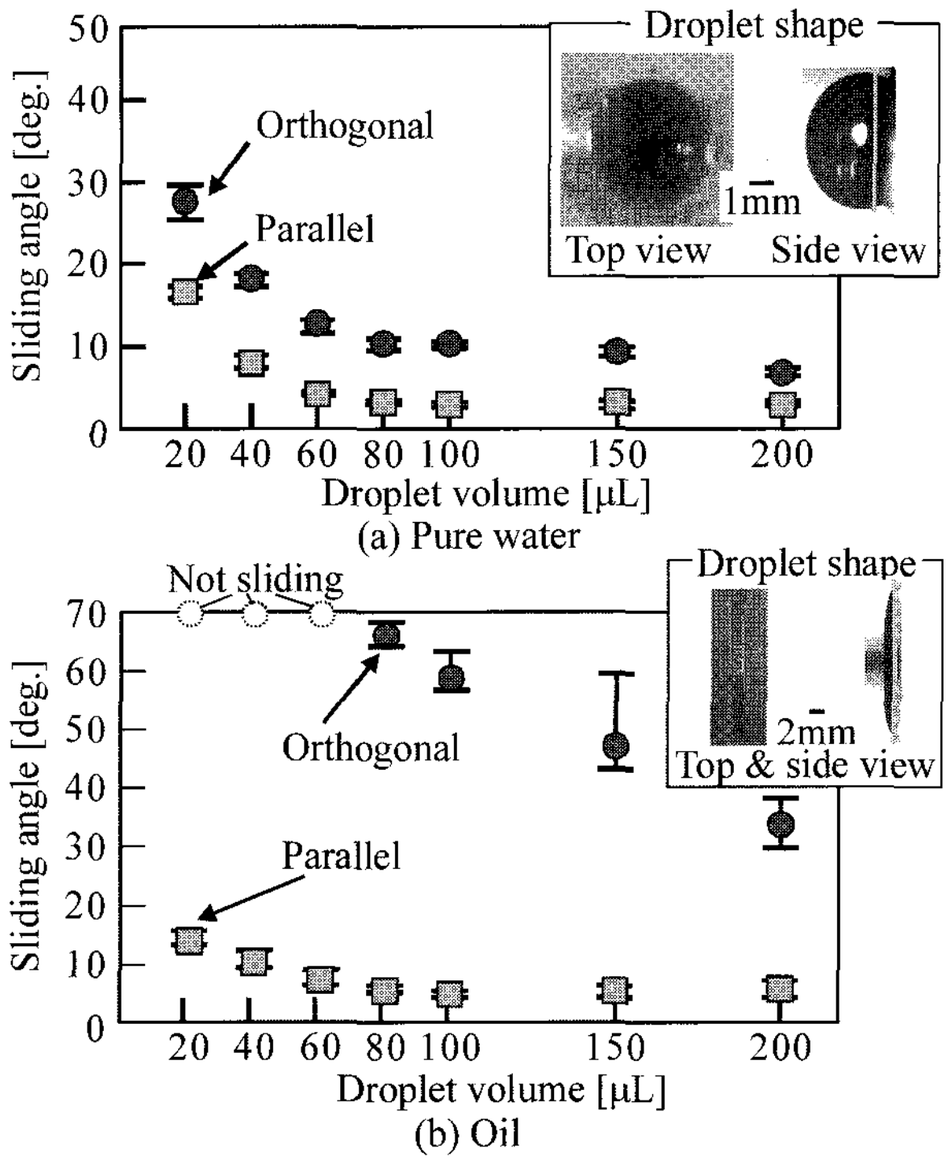

Fig. 5 Relationship between the droplet volume and the sliding angles (Structure No. 1)

The structure had a larger effect for oil, shown in Fig. 5(b). When the volume was less than 80 μL, the sliding angle orthogonal to the structure was greater than 70 degrees, which was the limit of the apparatus. On the other hand, the sliding angle parallel to the structure was 10 degrees. These results can be explained by the spreading of the droplet on the structure. The droplet shapes of pure water and oil are shown in the inset images in Fig. 5. The oil droplet spread along a groove, forming an elliptical shape, while the pure water droplet formed a circular shape spanning several grooves. The reasons for the elliptical shape of the oil droplet were its low surface tension and large capillary force, f, which, for a single channel, is given as follows:[10]

$$f = \gamma_{LV} A \cos\theta \tag{4}$$

where A is the contour length of the liquid-solid boundary. This formula cannot be applied directly because it is applicable only to a closed channel. However, it is easy to predict that such a deformed droplet has a strong directionality of mobility. Since the contact angle of an oil droplet is small (53 degrees) and the capillary force $f > 0$, it spreads easily along the direction parallel to the grooves.

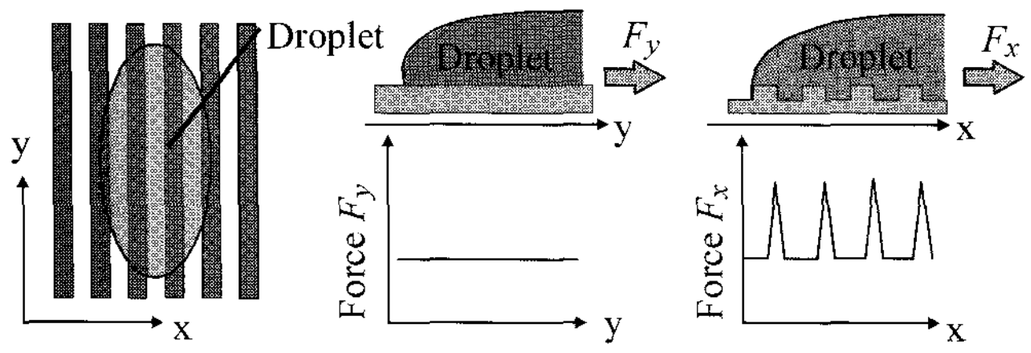

Fig. 6 Schematic representation of the sliding directionality

Figure 7 shows the relationship between the pitch P and the sliding angles for both water and oil. The broken line indicates the sliding angle on a flat surface. The droplet volume was maintained at 50 μL throughout the tests. The sliding angle on the structured surface tended to be smaller than that on the flat surface for pure water, shown in Fig. 7(a). The narrow pitch lowered the sliding angle since air was trapped in the grooves. In such cases, the fraction of the solid surface in the apparent contact area given by Eq. (2) decreased and the contact angle increased. When air is trapped, the sliding angle tends to be small. However, when the pitch P was as large as 2000 μm, the directionality increased. Here, the pitch and width of the grooves were large enough to contain the droplet. Therefore, the sidewall of the groove constrained the movement of the droplet.

The directionality of the sliding angle was strongly independent of the pitch size for oil, shown in Fig. 7(b). The sliding angle orthogonal to the structure increased beyond 70 degrees, which is the limit of the apparatus, except when $P = 2000$ μm.

Figure 8 shows the relationship between the height H and the sliding angles. The sliding angles decreased with increasing H for pure water, shown in Fig. 8(a). The sliding angle when $H = 15$ μm was larger than that of the flat surface in both sliding directions. Top views of the droplets on a horizontal substrate are also shown in the figure. It should be noted that the projected areas of the droplets were different although their volumes were the same. This difference suggests that air was trapped at the interface when $H = 100$ μm, while the droplets spread or penetrated into the grooves when $H = 15$ μm. When the droplets spread in the grooves, a pinning effect occurred and the motion of the droplet was constrained, thus increasing the sliding angle.

The effect of the height was remarkable and the sliding angles orthogonal to the structure were large for oil, shown in Fig. 8(b), due to the distorted droplets. As described above, oil droplets spread into the grooves with ease and then formed thin elongated shapes. Thus, they had strong directionality in their mobility. The contour length of the liquid-solid boundary was thin and long for $H = 100$ μm. Therefore, the sidewalls could be expected to constrict the motion.

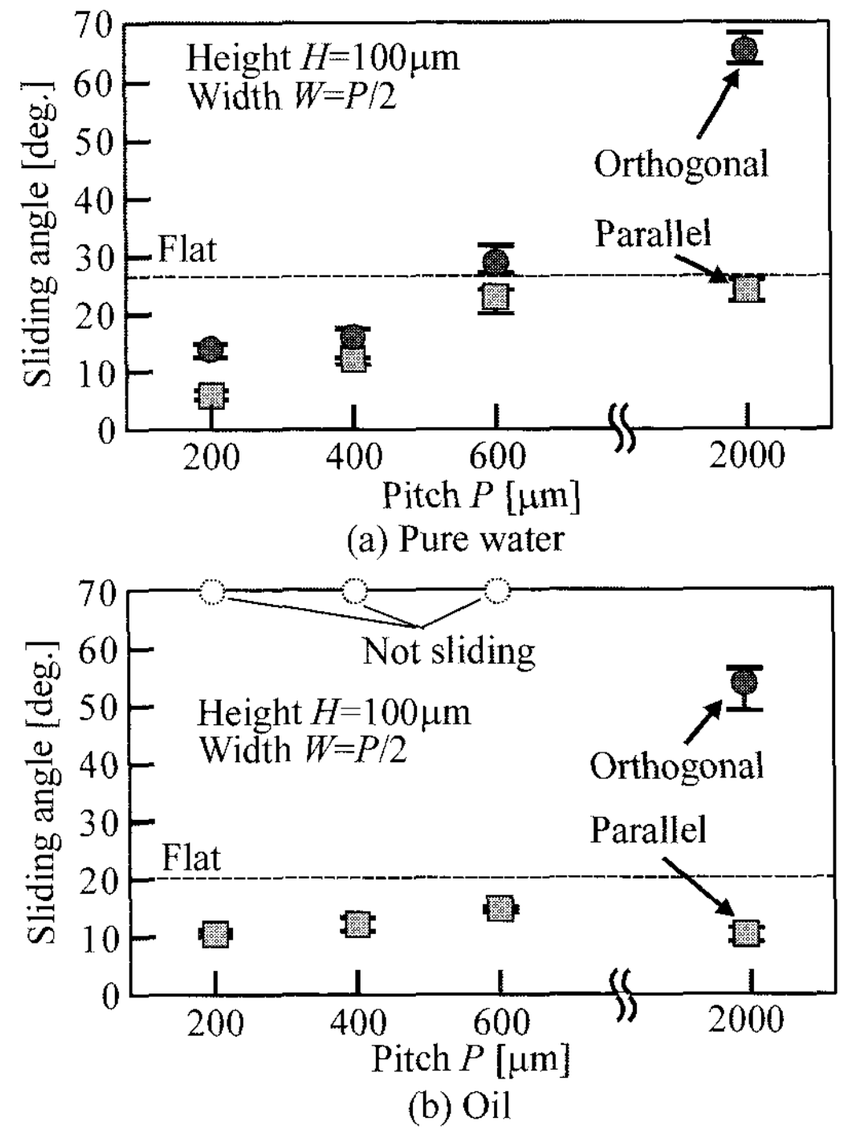

Fig. 7 Relationship between pitch P and sliding angles (Structures No. 1, 2, 3, and 4)

The sliding angle of oil had a different tendency from that of pure water. This strong directionality should be taken into consideration in the design of functional surfaces.

From the above results, the sliding angle, which is the main topic in previous studies,[1-4] can be designed by changing the groove dimensions and arrangement. However, it is also necessary to perform experiments with a large amount of liquid to identify actual design guidelines. In the set-up described above, the droplet size was limited owing to the syringe size and the stage stroke. Therefore, another apparatus was prepared.

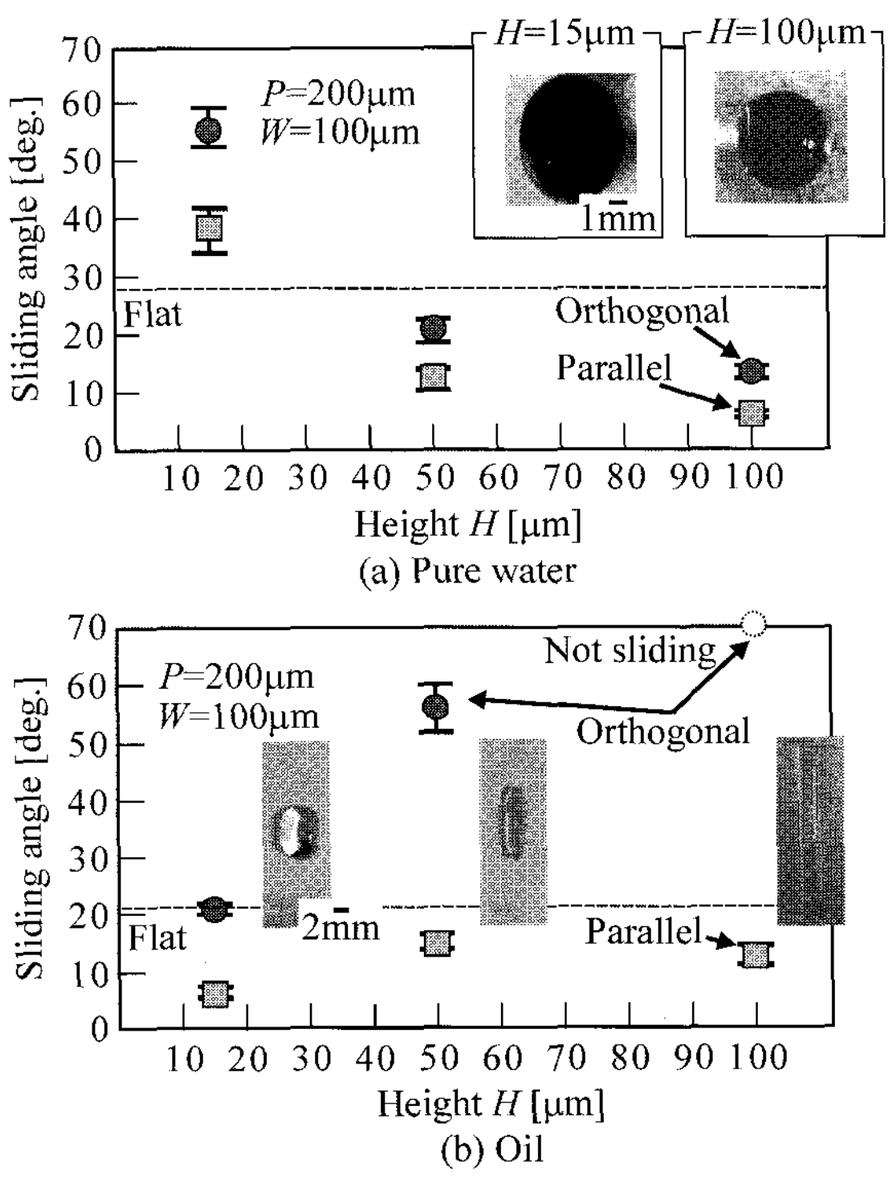

Fig. 8 Relationship between height H and sliding angles (Structures No. 1, 5, and 6)

4.2 Poured liquid

The poured-liquid apparatus, shown in Fig. 9, was prepared and a large amount of liquid was poured on the structured surfaces so that

the removal process could be observed. The substrate with the L&S structure was set on a frame to which a reservoir was attached. The reservoir contained 3 mL of pure water or oil. A rotation motor-stage inclined the frame according to commands received from a personal computer (PC). A CCD camera set on the same frame captured the images of the substrate.

The experimental procedure was as follows. First, the substrate was aligned vertically with the reservoir located at the lower end. Then, the stage was turned so that the liquid was poured on the substrate at an angle of $\varphi = 30$ degrees. The camera captured images at a constant interval just after the liquid was spattered to record the residual liquid on the substrate with time. The images were then analyzed to calculate the residual area of the liquid. The substrate area was 36 mm × 24 mm (864 mm^2). This evaluation method is more practical than conventional sliding angle techniques because the liquid volume is large and the residue can be directly observed.

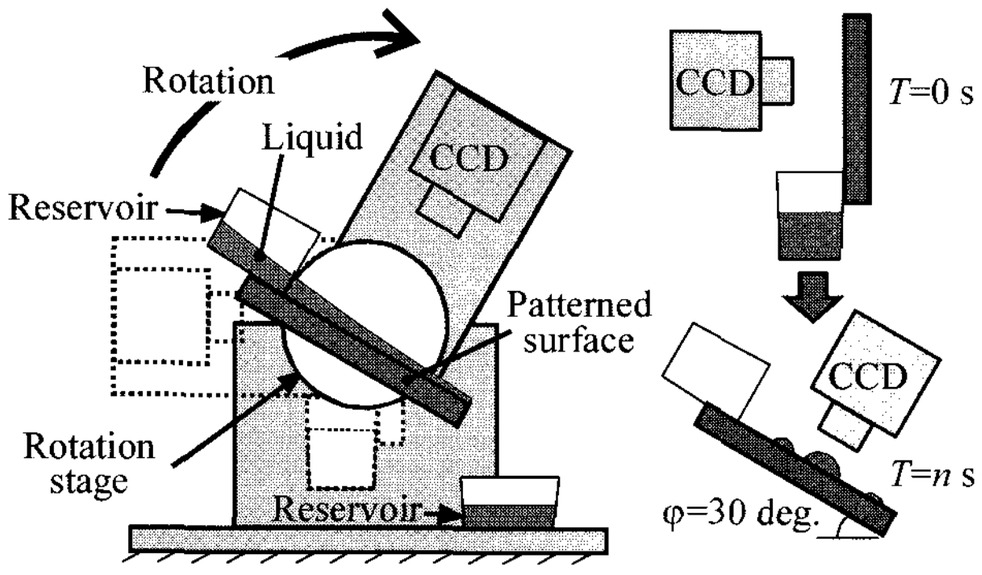

Fig. 9 Apparatus for the liquid spatter test

Figure 10 shows the relationship between the pitch P and the residual area of pure water, including the effect of the structural arrangement or orientation. The vertical axis denotes the average residual area after 10 repetitions. The photographs shown in the figure were taken just after the spatter of pure water. The effect of the pitch P on the residual area was small. However, the parallel arrangement could minimize the residual liquid on the substrate, while considerable liquid remained on the flat substrate. This tendency corresponds well with the sliding angle test results shown in Fig. 7. The small droplets remained sparsely distributed on the flat surface and the orthogonal grooves. Their estimated volumes were a few microliters, and they did not slide further down the surface because of the relatively large adsorption force compared to gravity. No droplets were observed on the substrate with the parallel grooves.

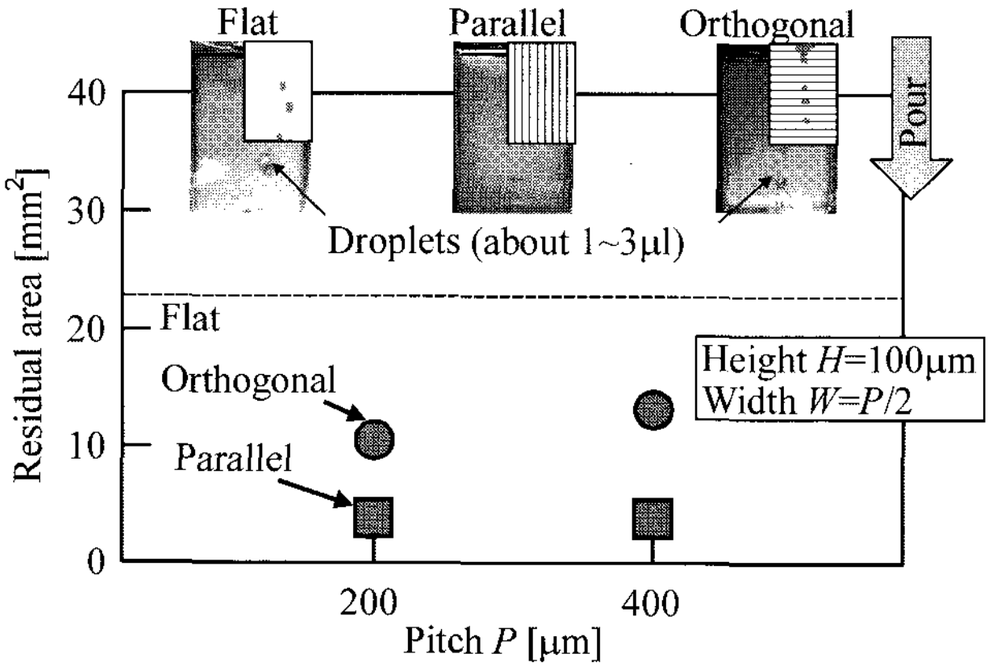

Fig. 10 Relationship between pitch P and residual area just after spattering of pure water (Structures No. 1 and 2)

Figure 11 shows the relationship between the pitch P and the residual area of oil just after the spatter, including the effect of the structural arrangement. In this case, both the effects of the pitch P and the arrangement were small. The oil spread over almost the entire substrate forming a thin film, as shown in the schematic illustrations attached to the photographs in which the regions of oil film are gray. However, the residual areas changed with time when the substrates were maintained at the same inclination.

Figure 12 shows the relationship between the elapsed time after the spatter and the residual areas. The residual area decreased with time for all the substrates. The residual area on the substrate with parallel grooves decreased much more rapidly than the other arrangements. The final residual area on substrate with orthogonal grooves was the largest because thin films were trapped in the grooves.

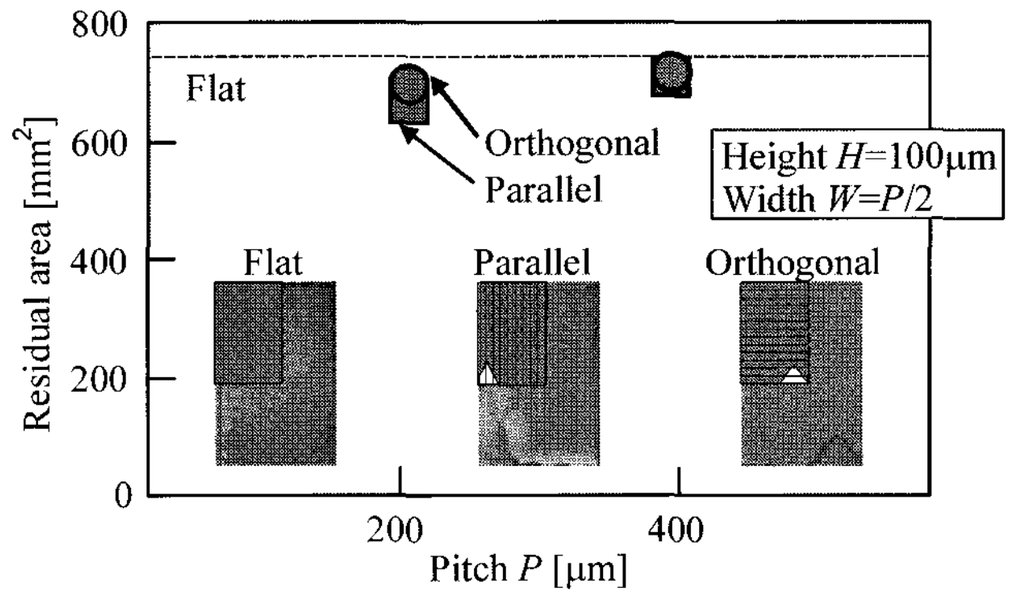

Fig. 11 Relationship between the pitch P and residual area just after spattering of oil (Structures No. 1 and 2)

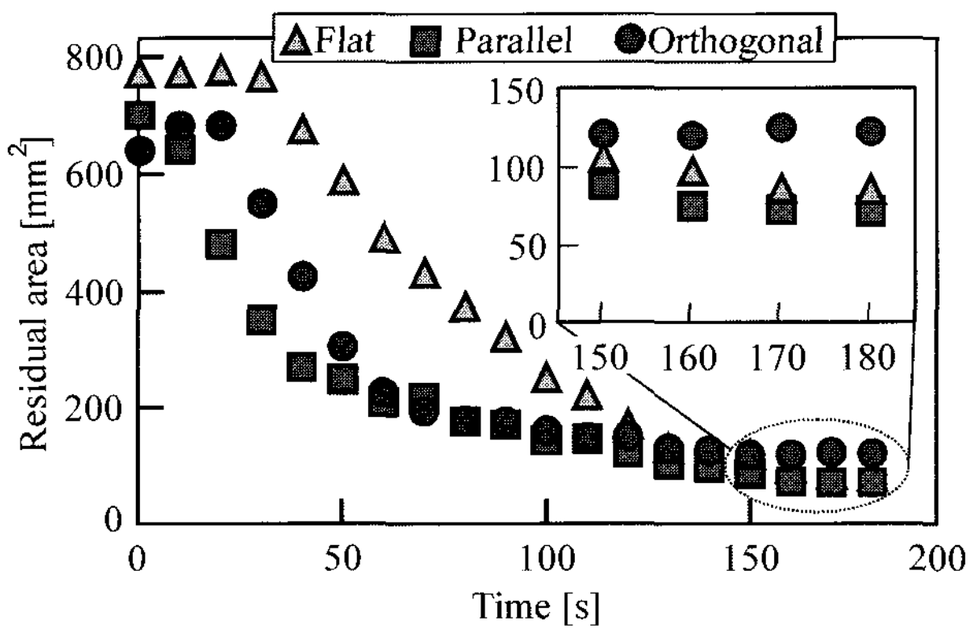

Fig. 12 Relationship between the elapsed times and residual areas

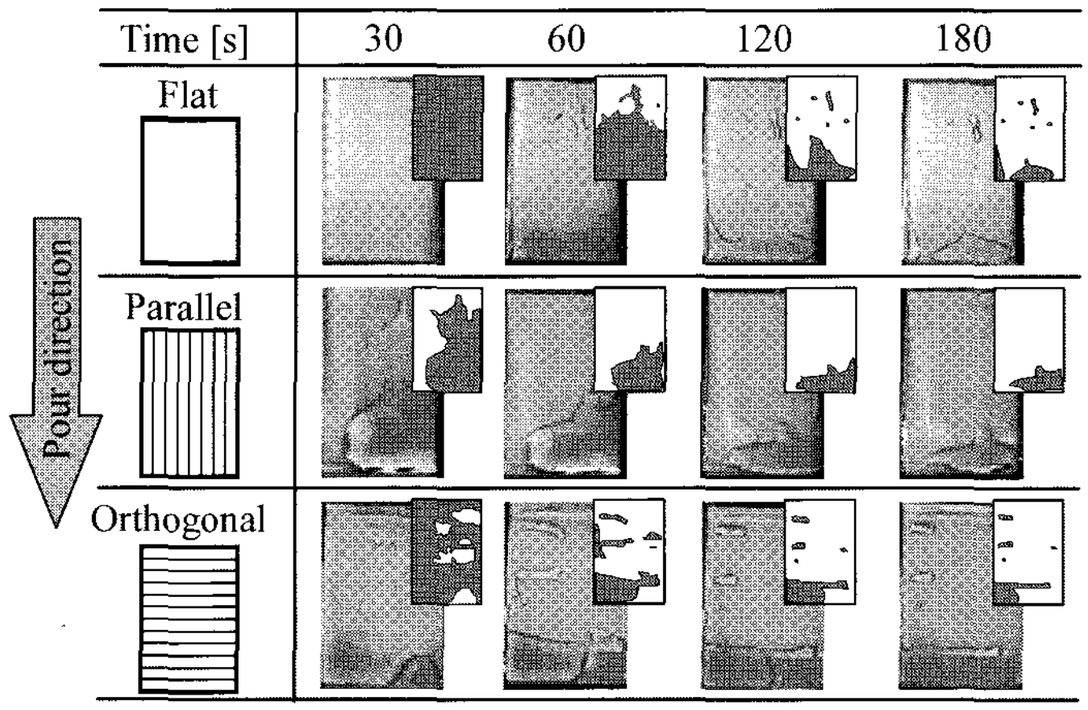

Fig. 13 Photographs of the substrate after spattering (Structure No. 1)

Figure 13 shows the typical time history of the substrate after spattering oil. The quality of the photographs was poor; hence sketches are included in the figure. A thin film was formed on the flat surface that slid down due to gravity. Droplets were formed instead of film for the parallel and orthogonal groove arrangements because of the weak repellent characteristic of the surface. For the parallel groove arrangement, large droplets slid down without leaving small droplets on the substrate. However, small droplets remained after the

major droplets had slid down for the orthogonal arrangement. In this case, the droplets spread wide in the grooves so that it was difficult for them to slide, as shown in Fig. 7(b).

It was inferred from the above results that the parallel arrangement was most effective in removing the liquid while the orthogonal arrangement was most effective in retaining the liquid on the surface.

5. Conclusions

This paper considered the mobility of droplets on a structured surface. First, the sliding angle was measured on line-and-space structures. Then, poured liquid was observed after it was spattered on the surfaces and the residual areas were compared. The results may be summarized as follows.

(1) The sliding angle could be controlled by the structural design. For pure water, a narrower pitch such as P = 200 μm and a larger height such as H = 100 μm decreased the sliding angle.

(2) The directionality of the sliding angle could also be controlled by the structure. For pure water, a wider pitch such as P = 2000 μm strengthened the directionality of the sliding angle. For oil, a larger height such as H = 100 μm strengthened the directionality. However, it is difficult to design or estimate the behavior of surfaces with oil because of its low surface tension.

(3) When the liquid was poured, a parallel structure arrangement was effective both for water and oil.

The establishment of design guidelines is one of the future goals of this research.

REFERENCES

1. Ma, M. and Hill, M. R., "Superhydrophobic Surfaces," Current Opinion in Colloid & Interface Sci., Vol. 11, Issue 4, pp. 193-202, 2006.

2. Morita, M., Koga, T., Otsuka, H. and Takahara, A., "Macroscopic-Wetting Anisotropy on the Line-Patterned Surface of Fluoroalkylsilane Monolayers," Langmuir, Vol. 21, No. 3, pp. 911-918, 2005.

3. Moronuki, N., Ryu, K. and Kaneko, A., "Control of Wettability with Surface Texturing and its Application," Proc. of the ASPE 19th Annual Meeting, CD-ROM, 2004.

4. Narhe, R. and Beysens, D. A., "Nucleation and Growth on a Superhydrophobic Grooved Surface," Phys. Rev. Lett., Vol. 93, No. 076103, 2004.

5. Song, J. H., Sakai, M., Yoshida, N., Suzuki, S., Kameshima, Y. and Nakajima, A., "Dynamic Hydrophobicity of Water Droplet on the Line-Patterned Hydrophobic Surfaces," Surface Sci., Vol. 600, Issue 13, pp. 2711-2717, 2006.

6. Chen, Y., He, B., Lee, J. and Patankar, N. A, "Anisotropy in the Wetting of Rough Surface," J. Colloid Interface Sci., Vol. 281, Issue 2, pp. 458-464, 2005.

7. Sato K., Lee K., Nishimura M. and Okutsu K., "Self-Alignment and Bonding of Microparts Using Adhesive Droplets," International Journal of Precision Engineering and Manufacturing, Vol. 8, No. 2, pp. 75-79, 2007.

8. Kim, J. and Kim, C. J., "Nanostructured Surfaces for Dramatic Reduction of Flow Resistance in Droplet-Based Microfluidics," Proc. IEEE Conference MEMS, pp. 479-482, 2002.

9. Young, T., "An Essay on the Cohesion of Fluids," Phil. Trans. Royal Soc., Vol. 95, pp. 65-87, 1805.

10. Cassie, A. B. D and Baxter, S., "Wettability of Porous Surface," Trans. Faraday Soc., Vol. 40, pp. 546, 1944.

11. Ichikawa, N., Hosokawa, K. and Maeda, R., "Interface Motion of Capillary-Driven Flow in Rectangular Microchannel," J. Colloid Interface Sci., Vol. 280, Issue 1, pp. 155-164, 2004.